International Journal of Engineering

Journal Homepage: www.ije.ir

The Effect of Rapid Deformation Process to Improve Creep and Tensile Resistance of AZ91 Magnesium Alloy Plates

H. Agha Amini Fashami[a], N. Bani Mostafa Arab*[a], M. Hosseinpour Gollo[a], B. Nami[b]

[a] *Mechanical Engineering, Shahid Rajaee Teacher Training University, Tehran, Iran*
[b] *Materials Engineering, Shahid Rajaee Teacher Training University, Tehran, Iran*

PAPER INFO

Paper history:
Received 28 December 2019
Received in revised form 25 June 2020
Accepted 13 August 2020

Keywords:
Rapid Deformation Process
Multi-Pass Friction Stir Processing
Tensile Strength
Creep
AZ91 Alloy

ABSTRACT

Demand for increasing strength to weight ratio, elimination of electromagnetic waves, and vibration damping has led to the wide application of magnesium-base alloys such as AZ91 in various industries like aerospace, military, vehicle, and shipbuilding. However, because of the unstable secondary particles and casting defects located on the rough grain boundaries and in the dendritic regions, due to sliding of the grain boundary, the creep resistance and tensile strength of Mg alloys at high temperatures reduce. To improve the high-temperature properties, rapid deformation processes such as friction stir processing can be employed. In this study, the influence of multi-pass friction stir processing on microhardness, tensile, and creep behavior of AZ91 at several temperatures from 25 to 210 °C has been studied. Optical microscopy and scanning electron micrograph were used to study the microstructure of the cast and processed samples and Clemex commercial software was used for grain size measurement. The experimental results indicated that at room temperature, the microhardness, tensile, and creep strength of the processed samples as compared to the unprocessed ones increased by 23, 29 and 38%, respectively. In addition, after multi-pass friction stir processing, the tensile and creep strength of the samples at 210 °C increased by 31 and 47%, respectively. Also, the average grain size of the multi-passed friction stir processed AZ91 alloy decreased by 88%. The maximum ultimate tensile strength of 276 MPa was obtained at the tool rotational speed of 1200 r/min, the traverse speed of 60 mm/min, and the tool tilt angle of 3°. The empirical results indicated that this rapid deformation process can be useful in enhancing the mechanical properties of AZ91 alloy at high temperatures.

***doi**: 10.5829/ije.2020.33.10a.22*

1. INTRODUCTION

Among the magnesium alloys, the AZ family has excellent properties such as castability at room temperature. However, $Mg_{17}Al_{12}$ particles with the low melting point (120 °C) on the rough grain boundaries and in the dendritic regions reduce the mechanical properties of these alloys at high temperatures. Friction stir processing (FSP) is a process to improve the tribological and microstructural properties of metallic materials. During FSP, sufficient heat is created to soften the material without melting which causes dynamic recrystallization of rough grains. In fact, due to the mechanical turbulence and stirring action using a rotating tool, the high strain rate deformation occurs. Therefore, FSP should cause a homogeneous microstructure, breakdown of the grains, decrease the size of $Mg_{17}Al_{12}$ eutectic particles, distribute the particles on the grain boundaries, reduce the casting defects and hence improve the mechanical properties [1]. However, the improvement of properties after FSP is highly dependent on the process parameters such as tool rotational speed, traverse speed, axial force, tool dimension and tool tilt angle. Recently, several works attempted to develop the performance of this process and increase the mechanical properties via FSP.

In recent years, many researchers [2-7] have demonstrated the effect of single-pass FSP on the mechanical properties of different alloys, especially cast

*Corresponding Author Institutional Email: *n.arab@sru.ac.ir* (N. Bani Mostafa Arab)

Please cite this article as: H. Agha Amini Fashami, N. Bani Mostafa Arab, M. Hosseinpour Gollo, B. Nami, The Effect of Rapid Deformation Process to Improve Creep and Tensile Resistance of AZ91 Magnesium Alloy Plates, International Journal of Engineering (IJE), IJE TRANSACTIONS A: Basics Vol. 33, No. 10, (October 2020) 2039-2046

alloys. Buffa et al. [8] reported the effect of water-cooling FSP on microstructure and tensile properties of 304L stainless steel. Their empirical and numerical reports indicate that water cooling increased the strength and reduced the ductility of the material; especially in the thermomechanically-affected zone (TMAZ). Cavaliere and Marco [9] stated that after single-pass FSP on AZ91, the superplasticity behavior improved. Feng [10] reported that single-pass FSP increased the tensile stress of AZ91 alloy at room temperature.

According to Sun and Apelian's research [11], after performing FSP on aluminum alloy, the size of secondary particles reduced, but the microstructure was not homogenous. Raja and Pancholi [12] reported after single-pass FSP on AZ91 alloy, the coarse structure of the α-Mg field refined slightly, the network of secondary particles dissolved, and the mechanical properties (such as tensile and impact) at room temperature improved. Lua and Zhangb. [13] reported that after FSP, the β-$Mg_{17}Al_{12}$ networks broke into smaller particles, but the microstructure of AZ91 alloys was not finely equiaxed.

Heidarpour et al. [14] investigated the microstructure and tensile properties of AZ91 after water-submerged FSP and non-cooled FSP. Their results show that after FSP, the rough casting structure converted into coaxial grains, and the lattice $Mg_{17}Al_{12}$ eutectic phases converted into pin-like particles on the grain boundaries. The structure of water-submerged FSP samples was more homogenous than that of the non-cooled processed samples; however, the ductility of the specimens after submerged FSP dramatically reduced. Edwin and Shamsudeen [15] studied the effect of tool pin length on microstructure and tensile strength during single-pass FSP. Their report shows that with increasing the pin length, tensile strength improved. However, increasing the length of the pin causes the tool to break quickly. Govindaraju et al. [16] studied the microstructure and mechanical properties of friction stir processed AZ91D with different heat treatment conditions. Wang et al. [2] conducted FSP on as-cast AZ31 to refine grains, homogenize the microstructure, and dissolve the secondary phases. Wang et al. [17] found that after FSP on Mg alloy, with dissolving the rough phases, the tensile and ductility properties were increased.

Mamaghani et al. [18] studied the effect of types of nanoparticles and process parameters on morphological and hardness properties of acrylonitrile butadiene styrene (ABS) plates. For this purpose, a slot with given dimensions (the depth and width) was created on the ABS sheets, and then three types of nanoparticles "nano clay, nano Fe_2O_3, and multi-walled carbon nanotube" were added to the slot. The workpieces were friction stir processed under different rotational and traverse speeds.

In addition, some researchers investigated the effective strain [19], temperature field [20, 21], microstructural modification [22] and material flow [23, 24] during single-pass FSP and friction stir welding (FSW) using 2-dimensional and 3-dimensional numerical modeling. Nie et al. [25] investigated the residual stresses and temperature field during FSW. Richards developed their model using two separate heat sources defined with Fortran77 DEFLUX subroutines. The modified model has been used to predict the thermal field around the tool [26]. Tutunchilar et al. [23] modeled the flow of material when a cylindrical pin was used for performing this process. They investigated the material behavior with the point tracking method. Rahul et al. [24] showed that during FSP on Mg alloys, the material flow around the pin is asymmetric. Assidi et al. [27] used 3D Forge3 finite element software based on Arbitrary Lagrangian-Eulerian formulation and automatic remeshing for modeling FSP.

Also, in recent years, FSP has been introduced as a relatively new way to create a homogeneous and fine-grained coating with improved resistance to wear and corrosion. Mostafapour et al. [28] studied the deposition of Al7075-T6 coating on Al2024-T351 substrates and investigated the effects of the rotational speed, axial force, and feed rate on the mechanical properties and microstructure of the specimens. Vahdati et al. [29] investigated the production of Al7075 surface composites using reinforcing particles (Al_2O_3) and FSP process.

Previous studies show that during single-pass FSP, thermal accumulation and asymmetric material flow applied to the samples may result in the growth of the grains adjacent to the process regions, non-homogenous structure, and imperceptible increase or reduction of mechanical properties. It is possible to prepare finer-grain specimens with improved strength and produce modified wide plates through multi-pass friction stir processing (MPFSP). In this section, some studies on performing MPFSP were reviewed. Chai et al. [30] subjected AZ91 plates with a thickness of 6 mm to two-pass FSP. Their results show that some coarse β-$Mg_{17}Al_{12}$ phases that existed after the first pass of FSP break and dissolve into the matrix under the action of the second pass of FSP. Lu et al. [31] conducted two-pass FSP (with water cooling) on cast AZ91 plates. Their results show that the microhardness, tensile strength, and elongation of the processed specimens were 94.7 HV, 155.5 MPa, and 31.5%, respectively, which were more than that of the base plates. Allavikutty et al. [32] developed a layered microstructure with three different configurations by MPFSP on AZ91 using three various tools with probe lengths of 4, 5, and 7 mm. The configurations were half thickness processed, surface modified, and full

thickness processed. They concluded that the fatigue properties improved with increasing the fraction of the friction stirred processed regions in AZ91 alloy.

Alavi et al. [33], studied the influence of overlapping ratio on graining, ductility, and tensile strength at room temperature after performing water-cooling FSP on AZ91. Mansoor and Ghosh [3], carried out the MPFSP on extruded ZK60 Mg plates to improve the mechanical properties. Nakata et al. [34] reported after MPFSP on A383 plate, the casting defects eliminated, microstructure refined, and ductility improved.

Sato and Park [4], mentioned that MPFSP is a process for the modification of AZ91 casting. Venkateswarlu et al. [35] investigated the effect of overlapping ratio(OR) and processing direction on the improvement of the tensile and ductility of AZ31 alloy.

Xicai et al. [5], conducted the two-pass FSP (with water cooling) on AZ61 magnesium alloy to improve the microstructure and dissolution of the β-phases. However, due to the adverse effect of texture evolution, the tensile strength of the two-pass processed workpiece compared to friction stir processed samples decreased.

A review of previous studies shows that the effect of consecutive passes (more than two passes) on mechanical properties and microstructure modification of AZ91 at high temperatures has not yet been investigated. As explained, in recent years, FSP has been the subject of many research studies. However, few studies have been conducted on MPFSP as a process to modify wide surfaces. In this research, the effect of MPFSP with 50% OR on microstructure, microhardness, tensile, and creep strength of AZ91 alloy at several temperatures from 25 to 210 °C were investigated. In the next sections, the description of materials, equipment, and tests are presented. In section 3, the results and discussion are presented and at the end, in section 4, conclusions are given.

2. MATERIALS AND METHODS

The workpiece material selected for this study was magnesium alloy AZ91 in the form of casting plates with the dimensions of 600×300×10 mm. The chemical composition of this alloy is listed in Table 1. The physical and mechanical properties of AZ91 are given in Table 2 [5, 36]. The tool was prepared from H13 tool steel with a pin size of 4mm diameter, 4mm length, and a flat shoulder with the diameter equal to 18mm. The tool properties are shown in Table 3 [37].

The tool was rotated clockwise and tilted 3 degrees opposite to the processing direction with 1mm of penetration depth. The process was performed using a universal milling machine DECKEL FP4M with

TABLE 1. The Chemical Composition of the AZ91 alloy

Al	Zn	Mn	Si	Fe	Ni	Mg
8.8	0.7	0.2	0.03	0.002	0.0002	Bal.

TABLE 2. The material properties of AZ91 at 25 ˚C

The important properties of AZ91	Value
"Young`s modulus of elasticity (GPa)"	46
"Poisson`s ratio"	0.33
"Thermal conductivity ($Wm^{-1}K^{-1}$)"	72
Coefficient of thermal expansion ($^0C^{-1}$)"	2.4×10^{-5}
Density (kg m^{-3})	1810
Specific heat capacity (J Kg^{-1} $^0C^{-1}$)	1050
Solidus temperature(^0C)	470
Liquids temperature (^0C)	595

TABLE 3. The material properties of H13

The essential properties of AZ91	Value
"Emissivity"	0.7
Coefficient of thermal expansion ($^0C^{-1}$)	1.17×10^{-5}
"Poisson`s ratio"	0.3

different rotational and traverse speeds. The traverse speeds were 40, 60, and 80mm/min. Also, the tool rotational speeds of 1000 and 1200 rpm were selected. To find suitable values for process parameters, the processed specimens were inspected for process defects. Small defects on the surface could be detected using the liquid penetrate test method according to the ASME-Section V standard (article 6). In addition, for the detection of internal defects, the radiography test according to EN1435 standard using panoramic XXG300s equipment was employed. Process defects were observed as shown in Figures 1 and 2. Finally, the rotational speed of 1200 rpm and the traverse speed of 60 mm/min were selected for producing defect-free samples. The friction stir processed workpiece, with the selected parameters is shown in Figure 3.

The OR is used to determine the overlapping area between two consecutive passes and is defined by Equation (1) [35].

$$OR = 1 - \left(\frac{l}{d_{probe}} \right) \quad (1)$$

where l and d_{probe} are "the distance between the centers of two consecutive passes" and "the pin diameter", respectively. After performing MPFSP on AZ91 plates with the selected parameters, the optical microscopy (OM, OLYMPUS CKX53 model) and scanning electron

microscopy (SEM, VEGA TESCAN-XMU model) were used to study the microstructure of the processed samples. In addition, the Vickers microhardness of the samples was measured on the cross section perpendicular to the processing path under 100 g loading for 15 s.

Standard tensile test specimens with 20mm length and the width of 6mm were cut using wire cut electro-discharge machining according to the ASTM standard E8/E8M [38]. These samples were parallel and perpendicular to the processing path (as shown in Figure 4). After preparing sub-size samples, the tensile tests were performed using the Zwick Roell testing device with the strain rate of 10^{-3} s^{-1}, at several temperatures of 25, 140, 170, and 210°C.

For conducting the impression creep test, the test samples with dimensions of 8×8×8 mm were prepared. The details of the impression creep test were explained by Mahmudi et al. [39]. The creep-testing device equipped with a controllable temperature furnace was used to carry out the constant-temperature, and constant-load impression creep tests with a simple cylindrical indenter having 2mm diameter. Also, the impression tests were performed at several temperatures (25, 140, 170, and 210°C).

Figure 1. Radiographic images with different rotational and progressive speeds

Figure 2. Defects detected by the penetrant test

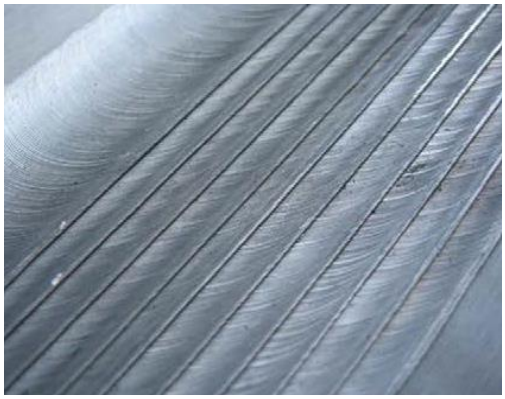

Figure 3. The friction stir processed workpiece with selected parameters

3. RESULTS AND DISCUSSION

3. 1. The Microhardness Test The hardness profiles in the stirred zone-up and stirred zone-down are shown in Figure 5. The profiles show that after MPFSP, generally, the hardness of processed workpieces increased to 87 VHN (Vickers hardness number), which was 23% more than the hardness of the base workpiece (71 VHN). As shown in Figure 5, the hardness of the stirred zone-up is more than the hardness of the stirred zone-down.

3. 2. The Microstructures The metallographic samples were prepared through the standard polishing method and then etched. The microstructure of the casting plates and multi-pass processed samples were studied using OM and SEM. The casting defects such as tunnels, grooves, cavities, and nonadhesion between the field and secondary particles are observed in Figure 6a. In addition, Figure 6b shows the microstructure of the cast workpiece that consists of non-homogenous grains and the network of eutectic phases in the α-Mg field.

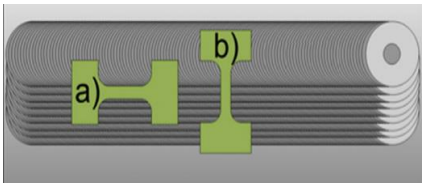

Figure 4. Cutting direction of the tensile test samples (a) Parallel and (b) perpendicular to the process path

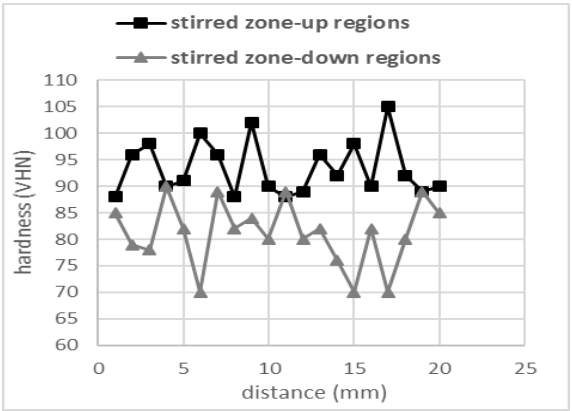

Figure 5. The hardness profiles in the stirred zone-up and stirred zone-down

After MPFSP, the microstructure refined, the grain size decreased, the eutectic lattice phases converted into the spherical shape particles, and the casting defects reduced as shown in Figure 7. After MPFSP, as shown in Figures 7b and 7c, the microstructure was non uniform. Because of intense deformation at the tool shoulder-workpiece interface, grains in the stirred zone-up can be coarser than those in the stirred zone-down, and the dislocations density in stirred zone-up is more than that in the stirred zone-down [40]. Since the microhardness of the processed samples is affected by the microstructural properties, dynamic recrystallization, texture changes, and especially the dislocations density [40]; therefore, the hardness in the zone-up is more than that in the stirred zone-down.

The average grain size of cast samples is about 98 µm. During FSP, the grains are refined. The average grain size of the MPFS Processed AZ91 alloy is about 11 µm and homogenous grains with reduced casing defects were observed. The CLEMEX commercial software was used for grain size measurement.

In a similar paper, El-Danaf et al. [41] investigated the effect of FSP on the grain size of cold-rolled sheets of AA5083. They reported that decreasing the grain size causes increase in hardness from 80 to 95HV on the nugget center. Nascimento et al. [42] studied the effect of FSP on the aluminum alloy (AA5083) for obtaining a uniform hardness using one-pass and multi-pass processes.

3. 3. Tensile Test The tensile test results for the base metal and the processed samples are given in Figure 8. As shown, the yield and ultimate stresses of the single-pass and MP processed samples at room temperature (parallel to the processing paths) increased by about 21 and 29% compared to the base workpiece. Improving the mechanical properties of the processed samples can be attributed to the refinement of the grains size in the processed zone and modifying the microstructure after MPFSP. In a similar research on AZ31, Feng and Ma [10] concluded that reducing the grain size increases strength. On the other hand, the recrystallization process reduces the density of dislocations. The competition between reducing the strength caused by decreasing the dislocations density and increasing the strength caused by reducing the grain size affects the hardness and tensile properties. In this research, the effect of reducing grain size is more effective, and the strength increased. Besides, after performing FSP, because of the elimination of defects and crushing of the unstable lattice intermetallic phases into the matrix, the microstructure and mechanical properties, especially at high temperatures improved. As shown in Figure 8, the yield and ultimate stresses of multi-pass processed samples at 140, 170, and 210°C increased by about 23 and 31% compared to the base workpieces. Reducing the tensile strength at a perpendicular direction to the processing path can be due to the development of firm basal texture in several non-perpendicular directions [43].

3. 4. Creep Test The creep behavior of base workpiece and the processed samples was investigated by impression testing in which the indenter is a circular cylinder with a flat end. After loading, the penetration depth of the indenter was measured automatically depending on time up to 4000s. The power-law equation defines the creep rate in the steady-state stage. When the impression test is used to determine creep resistance, the strain creep rate is calculated using the "impression depth of indenter"/time slope (V_{imp}=dh/dt) and equivalent stress is defined using the relation between the force applied to the punch and diameter of indenter

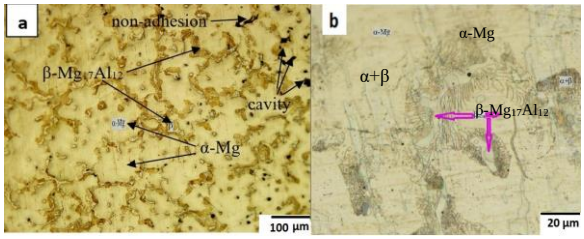

Figure 6. Unprocessed specimen of AZ91 alloy

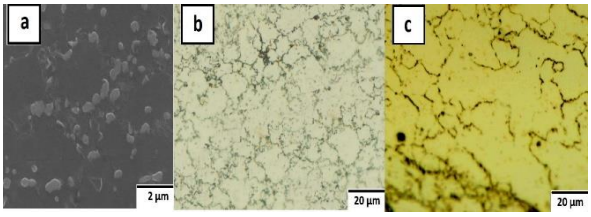

Figure 7. The microstructure of a) processed specimen of AZ91 alloy using SEM, b) stir zone-down region, c) stir zone-up region

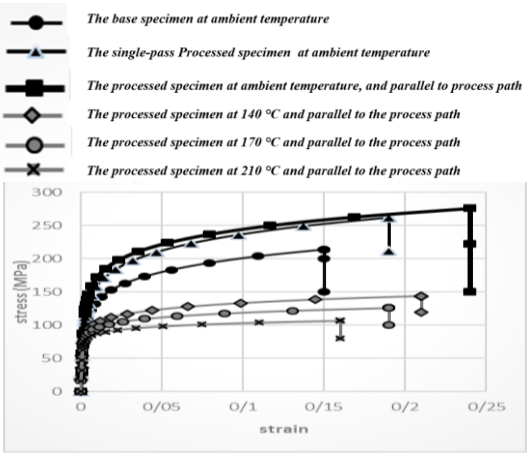

Figure 8. The Stress-strain diagrams for all sample

($\sigma_{imp} = 4F/\pi\varphi^2$). Here, F is the load and φ is the indenter diameter. Using the above equations and rearranging the power-law equation, the impression creep can be characterized by Equation (2).

$$\frac{V_{imp}T}{G} = A\left(\frac{\varphi c_2}{c_1^n}\right)\left(\frac{b}{d}\right)^p\left(\frac{bD_0}{k}\right)^n\left(\frac{\sigma_{imp}}{G}\right)^n \exp\left(\frac{Q_C}{RT}\right) \quad (2)$$

A: The constant,
b: The burgers vector,
d: The grain diameter,
D_0: The frequency index,
K: The Boltzmann's constant,
n: The stress exponent,
Qc: The creep-activation energy,
R: The universal gas constant.

Using this equation, to calculate the stress exponent n, the curve of $\ln(V_{imp}T/G)$ against $\ln(\sigma_{imp}/G)$ at constant T is plotted. Also, the activation energy Qc can be evaluated from a curve of $\ln(V_{imp}T/G)$ against (1/T) at constant (σ_{imp}/G). The shear modulus in this equation depends on the testing temperature. In this study, the creep of the base and processed samples is investigated at several temperatures when the $\sigma_{imp}/G \sim 0.034$ is constant.

The "G (MPa) =18,460–8.2T (K)" is the relation to calculate the shear modulus (G) of the AZ91 magnesium alloy at different temperatures (T). Here, by calculating the impression depth/time slope in the steady-state stage, the effect of FSP and temperature on the creep rate can be investigated. Figure 9 shows the penetration depth of indenter at different times when the tests were performed at three temperatures of 140, 170, and 210°C on cast and friction stir processed specimens.

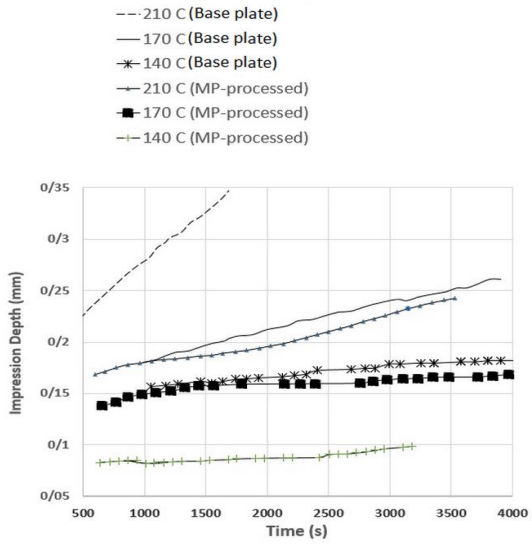

Figure 9. The plot of impression depth against time at temperatures of 140, 170, and 210 °C for casting and MPFS Processed specimens

As shown in Figure 9, based on the penetration rate of the indenter, creep strength of the processed specimens at 210, 170, and 140 °C are more than that of the unprocessed specimens by about 47, 36, and 33%, respectively. As shown in Figure 6, the microstructure of the cast specimen was found to be unstable due to the network of eutectic particles on the grain boundary during cooling. As shown in Figure 7, the size of grains decreased and β-particles dissolved in the matrix. Therefore, the negative effects of reducing the strength due to the softening of eutectic phases, especially at high temperatures is decreased.

4. CONCLUSIONS

According to the experimental results, the following conclusions could be given:

1. The microhardness of the processed samples is more than that of the base material by about 23%.
2. The microhardness in the stirred zone-up is more than that in the stirred zone-down by about 14%.
3. The yield and tensile strength of specimens after processing increased by about 21 and 29% compared to the base workpiece (at room temperature).
4. The main factors for increasing the tensile strength of the MPFSP samples are considered to be the casting and processing defects, homogenous microstructure, and dissolution of the β-phases.
5. Improvement of tensile and creep properties at high temperatures is far more significant than that at room temperature. The yield and ultimate stresses of multi-pass processed samples at 140, 170, and 210°C increased by about 23% and 31% compared to the base workpiece.
6. The creep resistance of friction stir processed samples was more than that of the unprocessed ones by about 38%.
7. The microstructure investigation shows that after FSP with the selected parameters, defects such as cracks, cavity, interconnection, non-adhesion between the field, secondary phase particles, and rough network phases, which cause stress concentration and lead to accidental and bad time failure are removed, and the microstructure is modified.

5. REFERENCES

1. Mordike, B. and Ebert, T., "Magnesium: Properties—applications—potential", ***Materials Science and Engineering: A***, Vol. 302, No. 1, (2001), 37-45. DOI: 10.1016/S0921-5093(00)01351-4
2. Wang, Y., Huang, Y., Meng, X., Wan, L. and Feng, J., "Microstructural evolution and mechanical properties of mgznyzr alloy during friction stir processing", ***Journal of Alloys***

and Compounds, Vol. 696, No., (2017), 875-883. DOI: 10.1016/j.jallcom.2016.12.068

3. Mansoor, B. and Ghosh, A., "Microstructure and tensile behavior of a friction stir processed magnesium alloy", ***Acta materialia***, Vol. 60, No. 13-14, (2012), 5079-5088. DOI: 10.1016/j.actamat.2012.06.029
4. Sato, Y., Park, S., Matsunaga, A., Honda, A. and Kokawa, H., "Novel production for highly formable mg alloy plate", ***Journal of Materials Science***, Vol. 40, No. 3, (2005), 637-642. DOI: 10.1007/s10853-005-6301-1
5. Luo, X., Cao, G., Zhang, W., Qiu, C. and Zhang, D., "Ductility improvement of an az61 magnesium alloy through two-pass submerged friction stir processing", ***Materials***, Vol. 10, No. 3, (2017), 253. DOI: 10.3390/ma10030253
6. Gangil, N., Maheshwari, S. and Siddiquee, A.N., "Influence of tool pin and shoulder geometries on microstructure of friction stir processed aa6063/sic composites", ***Mechanics & Industry***, Vol. 19, No. 2, (2018), 211. DOI: 10.1051/meca/2018010
7. Kordestani, F., Ghasemi, F.A. and Arab, N.M., "An investigation of fsw process parameters effects on mechanical properties of pp composites", ***Mechanics & Industry***, Vol. 17, No. 6, (2016), 611. DOI: 10.1051/meca/2016012
8. Buffa, G., Hua, J., Shivpuri, R. and Fratini, L., "A continuum based fem model for friction stir welding—model development", ***Materials Science and Engineering: A***, Vol. 419, No. 1-2, (2006), 389-396. DOI: 10.1016/j.msea.2005.09.040
9. Cavaliere, P. and De Marco, P., "Fatigue behaviour of friction stir processed az91 magnesium alloy produced by high pressure die casting", ***Materials Characterization***, Vol. 58, No. 3, (2007), 226-232. DOI: 10.1016/j.matchar.2006.04.025
10. Feng, A. and Ma, Z., "Enhanced mechanical properties of mg–al–zn cast alloy via friction stir processing", ***Scripta materialia***, Vol. 56, No. 5, (2007), 397-400. DOI: 10.1016/j.scriptamat.2006.10.035.
11. Sun, N. and Apelian, D., "Friction stir processing of aluminum cast alloys for high performance applications", ***Jom***, Vol. 63, No. 11, (2011), 44-50. DOI: 10.1007/s11837-011-0190-3
12. Raja, A. and Pancholi, V., "Effect of friction stir processing on tensile and fracture behaviour of az91 alloy", ***Journal of Materials Processing Technology***, Vol. 248, No., (2017), 8-17. DOI: 10.1016/j.jmatprotec.2017.05.001
13. Lu, Z.L. and Zhang, D.T., "Microstructure and mechanical properties of a fine-grained az91 magnesium alloy prepared by multi-pass friction stir processing", in Materials Science Forum, Trans Tech Publ. Vol. 850, 778-783. DOI: 10.4028/www.scientific.net/MSF.850.778
14. Heidarpour, A., Ahmadifard, S. and Rohania, N., "Fsp pass number and cooling effects on the microstructure and properties of az31", ***Journal of Advanced Materials and Processing***, Vol. 6, No. 2, (2018), 47-58. DOI: http://jmatpro.iaun.ac.ir/article_623137.html
15. Shamsudeen, S. and Dhas, J.E.R., "Optimization of multiple performance characteristics of friction stir welded joint with grey relational analysis", ***Materials Research***, Vol. 21, No. 6, (2018). DOI: 10.1590/1980-5373-mr-2017-1050
16. Govindaraju, M., Vignesh, R.V. and Padmanaban, R., "Effect of heat treatment on the microstructure and mechanical properties of the friction stir processed az91d magnesium alloy", ***Metal Science and Heat Treatment***, Vol. 61, No. 5-6, (2019), 311-317. DOI: 10.1007/s11041-019-00422-1
17. Wang, Q., Xiao, L., Liu, W., Zhang, H., Cui, W., Li, Z. and Wu, G., "Effect of heat treatment on tensile properties, impact toughness and plane-strain fracture toughness of sand-cast mg-6gd-3y-0.5 zr magnesium alloy", ***Materials Science and Engineering: A***, Vol. 705, (2017), 402-410. DOI: 10.1016/j.msea.2017.08.100
18. Mamaghani Shishavan, S., Azdast, T., Mohammadi Aghdam, K., Hasanzadeh, R., Moradian, M. and Daryadel, M., "Effect of different nanoparticles and friction stir process parameters on surface hardness and morphology of acrylonitrile butadiene styrene", ***International Journal of Engineering, Transactions A: Basics***, Vol. 31, No. 7, (2018), 1117-1122. DOI: 10.5829/ije.2018.31.07a.16
19. Asadi, P., Mahdavinejad, R. and Tutunchilar, S., "Simulation and experimental investigation of fsp of az91 magnesium alloy", ***Materials Science and Engineering: A***, Vol. 528, No. 21, (2011), 6469-6477. DOI: 10.1016/j.msea.2011.05.035
20. Swaminathan, S., Oh-Ishi, K., Zhilyaev, A.P., Fuller, C.B., London, B., Mahoney, M.W. and McNelley, T.R., "Peak stir zone temperatures during friction stir processing", ***Metallurgical and Materials Transactions A***, Vol. 41, No. 3, (2010), 631-640. Doi: 10.1007/s11661-009-0140-7
21. Yu, Z., Zhang, W., Choo, H. and Feng, Z., "Transient heat and material flow modeling of friction stir processing of magnesium alloy using threaded tool", ***Metallurgical and Materials Transactions A***, Vol. 43, No. 2, (2012), 724-737. DOI: 10.1007/s11661-011-0862-1
22. Shercliff, H.R., Russell, M.J., Taylor, A. and Dickerson, T.L., "Microstructural modelling in friction stir welding of 2000 series aluminium alloys", ***Mechanics & Industry***, Vol. 6, No. 1, (2005), 25-35. DOI: 10.1051/meca:2005004
23. Tutunchilar, S., Haghpanahi, M., Givi, M.B., Asadi, P. and Bahemmat, P., "Simulation of material flow in friction stir processing of a cast al–si alloy", ***Materials & Design***, Vol. 40, (2012), 415-426. DOI: 10.1016/j.matdes.2012.04.001
24. Jain, R., Pal, S.K. and Singh, S.B., "Finite element simulation of pin shape influence on material flow, forces in friction stir welding", ***The International Journal of Advanced Manufacturing Technology***, Vol. 94, No. 5-8, (2018), 1781-1797. DOI: 10.1007/s00170-017-0215-3
25. Nie, L., Wu, Y. and Gong, H., "Prediction of temperature and residual stress distributions in friction stir welding of aluminum alloy", ***The International Journal of Advanced Manufacturing Technology***, Vol. 106, No. 7-8, (2020), 3301-3310. DOI: 10.1007/s00170-019-04826-4
26. De Dear, R.J. and Brager, G.S., "Thermal comfort in naturally ventilated buildings: Revisions to ashrae standard 55", ***Energy and Buildings***, Vol. 34, No. 6, (2002), 549-561. DOI: 10.1016/S0378-7788(02)00005-1
27. Assidi, M., Fourment, L., Guerdoux, S. and Nelson, T., "Friction model for friction stir welding process simulation: Calibrations from welding experiments", ***International Journal of Machine Tools and Manufacture***, Vol. 50, No. 2, (2010), 143-155. DOI: 10.1016/j.ijmachtools.2009.11.008
28. Mostafapour, A., Moradi, M., Kamali, H. and Saleh Meiabadi, M., "Multi-response optimization of the mechanical and metallurgical properties of al7075-t6 deposition process on al2024-t351 by friction surfacing using rsm and the desirability approach", ***Iranian Journal of Materials Forming***, Vol. 7, No. 1, (2020), 100-115. DOI: 10.22099/IJMF.2020.35736.114
29. Vahdati, M. and Moradi, M., "Statistical analysis and optimization of the yield strength and hardness of surface composite al7075/Al_2O_3 produced by fsp via rsm and desirability approach", ***Iranian Journal of Materials Forming***, Vol. 7, No. 1, (2020), 32-45. DOI: 10.22099/IJMF.2020.35554.1143
30. Chai, F., Yan, F., Lu, Q. and Fang, X., "Microstructures and mechanical properties of az91 alloys prepared by multi-pass friction stir processing", ***Journal of Materials Research***, Vol. 33, No. 12, (2018), 1789-1796. DOI: 10.1557/jmr.2018.98

31. Lu, Z., Zhang, D., Zhang, W. and Qiu, C., "Microstructure and properties of az91 magnesium alloy prepared by multi-pass friction stir processing under different cooling conditions", ***Journal of Aeronautical Materials***, Vol. 36, (2016), 33-38. DOI: 10.11868/j.issn.1005-5053.2016.1.006
32. Allavikutty, R., Pancholi, V. and Mishra, B.K., Layered microstructure generated by multipass friction stir processing in az91 alloy and its effect on fatigue characteristics, in Proceedings of fatigue, durability and fracture mechanics. 2018, Springer.213-222. DOI: 10.1007/978-981-10-6002-1_17
33. Nia, A.A., Omidvar, H. and Nourbakhsh, S., "Effects of an overlapping multi-pass friction stir process and rapid cooling on the mechanical properties and microstructure of az31 magnesium alloy", ***Materials & Design***, Vol. 58, (2014), 298-304. DOI: http://jmatpro.iaun.ac.ir/article_623137.html
34. Nakata, K., Kim, Y., Fujii, H., Tsumura, T. and Komazaki, T., "Improvement of mechanical properties of aluminum die casting alloy by multi-pass friction stir processing", ***Materials Science and Engineering: A***, Vol. 437, No. 2, (2006), 274-280. DOI: 10.1016/j.msea.2006.07.150
35. Venkateswarlu, G., Devaraju, D., Davidson, M., Kotiveerachari, B. and Tagore, G., "Effect of overlapping ratio on mechanical properties and formability of friction stir processed mg az31b alloy", ***Materials & Design***, Vol. 45, (2013), 480-486. DOI: 10.1016/j.matdes.2012.08.031
36. Hasan, M. and Begum, L., "Semi-continuous casting of magnesium alloy az91 using a filtered melt delivery system", ***Journal of Magnesium and Alloys***, Vol. 3, No. 4, (2015), 283-301. DOI: 10.1016/j.jma.2015.11.005
37. Yuan, Y., Guo, Q., Sun, J., Liu, H., Xu, Q., Wu, Y., Song, D., Jiang, J. and Ma, A., "High mechanical properties of az91 mg alloy processed by equal channel angular pressing and rolling", ***Metals***, Vol. 9, No. 4, (2019), 386. DOI: 10.3390/met9040386
38. Standard, A., "E8/e8m-13a.(2013).“Standard test methods for tension testing of metallic materials.”", ***ASTM International***, Vol. 1, No. 1-27.
39. Mahmudi, R., Geranmayeh, A. and Rezaee-Bazzaz, A., "Impression creep behavior of lead-free sn–5sb solder alloy", ***Materials Science and Engineering: A***, Vol. 448, No. 1-2, (2007), 287-293. DOI: 10.1016/j.msea.2006.10.092
40. Miranda, R.M., Gandra, J.P., Vilaca, P., Quintino, L. and Santos, T.G., "Surface modification by solid state processing, Woodhead Publishing, (2013). ISBN: 9780857094698
41. El-Danaf, E.A., El-Rayes, M.M. and Soliman, M.S., "Friction stir processing: An effective technique to refine grain structure and enhance ductility", ***Materials & Design***, Vol. 31, No. 3, (2010), 1231-1236. DOI: 10.1016/j.matdes.2009.09.025
42. Nascimento, F., Santos, T., Vilaça, P., Miranda, R. and Quintino, L., "Microstructural modification and ductility enhancement of surfaces modified by fsp in aluminium alloys", ***Materials Science and Engineering: A***, Vol. 506, No. 1-2, (2009), 16-22. DOI: 10.1016/j.msea.2009.01.008
43. Cipoletti, D.E., Bower, A.F. and Krajewski, P.E., "Anisotropy in plastic deformation of extruded magnesium alloy sheet during tensile straining at high temperature", ***Integrating Materials and Manufacturing Innovation***, Vol. 2, No. 1, (2013), 81-100. DOI: 10.1186/2193-9772-2-4

Persian Abstract

چکیده

تقاضا برای افزایش نسبت استحکام به وزن، حذف امواج الکترومغناطیسی و میرایی ارتعاشات، باعث افزایش کاربردآلیاژ های منیزیم از جمله AZ91 در صنایع مختلف مانند هوافضا، نظامی، خودروسازی و کشتی سازی گردیده است. البته به دلیل حضور ذرات ناپایدار ثانویه در مرز دانه ها و مناطق دندریتی، استحکام کششی و مقاومت خزشی آلیاژهای منیزیم در دماهای بالا کاهش می یابد. برای بهبود این خواص در دمای بالا، از فرآیندهای تغییر شکل سریع مانند فرایند اصطکاکی اغتشاشی استفاده می شود. در این تحقیق، تأثیر فرایند اصطکاکی اغتشاشی چند پاسه بر میکروسختی، رفتار کششی و خزشی آلیاژ منیزیم AZ91 مورد بررسی قرار گرفته است. همچنین از تصاویر میکروسکوپهای نوری و الکترونی برای مطالعه ریز ساختار نمونه ها استفاده شده است. نتایج نشان می دهد که در دمای اتاق، میکرو سختی، استحکام کششی و مقاومت خزشی به ترتیب حدود ۲۳، ۲۹ و ۳۸ درصد بهبود یافته اند. همچنین پس از فرایند اصطکاکی اغتشاشی چند پاسه، استحکام کششی و خزشی در دمای ۲۱۰ درجه سانتیگراد به ترتیب ۳۱ و ٤٧ درصد افزایش یافت. بیشترین استحکام نهایی کششی برابر با ۲۷٦ مگا پاسکال در سرعت چرخشی ۱۲۰۰ دور در دقیقه، سرعت خطی ٦۰ میلیمتر بر دقیقه و زاویه ابزار ۳ درجه بدست آمد. نتایج تجربی نشان می دهد که فرایند چندپاسه می تواند دربهبود خواص مکانیکی آلیاژ در دماهای بالا مفید باشد.